



Epidermal growth factor receptor (EGFR) and neuregulin (Neu) activation in human airway epithelial cells exposed to nickel acetate

S. Giunta, A. Castorina, S. Scuderi, C. Patti, V. D'Agata *

Department of Bio-Medical Sciences, University of Catania, Catania, Italy

ARTICLE INFO

Article history:

Received 9 November 2011

Accepted 13 December 2011

Available online 21 December 2011

Keywords:

Nickel
Epidermal growth factor
Apoptosis
Airway epithelial cells

ABSTRACT

Nickel compounds are potential carcinogenic agents that produce a range of biological effects, including inhibition of cell death. Because suppression of apoptosis is thought to contribute to the initiation of carcinogenesis, we investigated the effects of nickel acetate (Ni^{2+}) treatment on apoptosis in two different airway epithelial cell lines (A549 and Beas-2B, respectively). Furthermore, since both the epidermal growth factor receptor (EGFR) and neuregulin (Neu) are involved in neoplastic development, mRNAs and expression levels of total and phosphorylated proteins (p-EGFR^{Tyr1173} and p-Neu^{Tyr1248}, respectively) were also measured. We found that exposure of A549 cells to Ni^{2+} resulted in significantly reduced cell viability, as well as increased apoptosis and DNA fragmentation at relatively low concentrations (0.1 and 0.5 mM) after 24 and 48 h. These changes were accompanied by reduced EGFR and Neu mRNAs and proteins, phosphorylated proteins as well as decreased Bcl-2 and increased BAX protein expression. Conversely, Beas-2B cells exposed to equivalent concentrations of Ni^{2+} did not show evident signs of apoptosis and DNA damage, hence showing increased expression and phosphorylation of both EGFR and Neu, increased Bcl-2 and reduced BAX expression. Altogether, our finding indicate that Ni^{2+} exposure differently affects apoptosis initiation either in non-tumorigenic (Beas-2B) and tumorigenic airway epithelial cells (A549), suggesting a potential involvement of EGFR/Neu receptors.

© 2011 Elsevier Ltd. All rights reserved.

1. Introduction

Occupational exposure to nickel compounds occurs in a variety of industrial processes. Aerosols of nickel salts are the types of exposure found in the electroplating and electrolysis areas of nickel refineries (Costa, 2002). However, the release of nickel into the environment represents a potential for nonoccupational exposure (Denkhaus and Salnikow, 2002). Nickel compounds can enter the body through inhalation, ingestion, and dermal absorption (Costa, 2002; Sivulka, 2005). Epidemiological studies have associated occupational exposure to nickel compounds to elevated incidence of cancer in the respiratory tract, such as nasal and lung cancer (Kasprzak et al., 2003). Studies performed both *in vitro* and/or using experimental animals *in vivo* have also confirmed the carcinogenic potential of nickel compounds (Kasprzak et al., 2003; Cangu et al., 2002). It has been reported that nickel compounds can regulate the expression of specific genes related to tumor development (Salnikow and Costa, 2000), however, the molecular mechanisms involved have not been clearly identified.

* Corresponding author. Address: Department of Bio-Medical Sciences, University of Catania, Via S.Sofia, 87, 95123 Catania, Italy. Tel.: +39 095 3782147; fax: +39 095 3782046.

E-mail address: vdagata@unict.it (V. D'Agata).

The epidermal growth factor (EGF) receptors belong to the subclass 1 of the receptor tyrosine kinase (RTK) superfamily. There are four EGF receptor family members: EGFR (ErbB1 or HER1), Neu (ErbB2 or HER2), ErbB3 (HER3) and ErbB4 (HER4). These receptors are situated at the cell membrane and have an extracellular ligand-binding region, a transmembrane region and a cytoplasmic tyrosine-kinase domain. Ligand binding to the receptors results in receptor homo- and hetero-dimers, activation of the intrinsic kinase domain and phosphorylation of specific tyrosine residues within the cytoplasmic tail. Proteins dock on these phosphorylated residues lead to the activation of a variety of intracellular signaling pathways that promote cell growth, proliferation, differentiation, and migration (Zandi et al., 2007; Olayioye et al., 2000; Baselga and Arteaga, 2005; Yarden and Sliwkowski, 2001). Cooperation between the various EGF receptors has been observed in oncogenic transformation both *in vitro* and in human primary tumors. In particular, both EGFR and Neu receptors seem to play a crucial role in the development of different neoplasms, acting either by promoting abnormal cell growth or by inhibiting apoptosis (Mosesson and Yarden, 2004).

Apoptosis is a physiological event that naturally occurs in cells, and once activated, may represent a protective mechanism against neoplastic development. In fact, aberrant disruption of the apoptotic function allows damaged or transformed cells to escape inappropriately from programmed cell death and potentially to proliferate,

further providing the initiating events that lead to cancer development (Wyllie et al., 1999; Liu et al., 2001; Correa and Miller, 1998). Several findings have reported that nickel compounds may either promote apoptosis or cell resistance in different cell types (Ahamed, 2011; Ding et al., 2006; Pan et al., 2011). These opposite effects might depend on the different activation of specific target membrane receptors and/or molecular pathways. In a previous work we have shown that exposure to hexavalent chromium induced changes in the expression of EGF receptors in human alveolar type 2-like epithelial cells (A549), suggesting a role of these receptors in metal-induced lung cancer development (Castorina et al., 2008). To date, however, it has not been established whether nickel exposure modifies EGFR/Neu receptors activation in airway epithelial cells.

In the present study we have hypothesized that (1) nickel acetate (Ni^{2+})-treatment might differently affect apoptosis initiation in two airway epithelial cell lines and that (2) Ni^{2+} -induced changes in the activation state of EGFR/Neu receptors might contribute to the diverse biological response. For this purpose, comparative analyses of cell viability, apoptosis, DNA damage, as well as the expression of the antiapoptotic protein Bcl-2 and the proapoptotic protein BAX were performed both in tumorigenic alveolar type 2-like (A549) and non-tumorigenic bronchial epithelial cells (Beas-2B) exposed to different concentrations of Ni^{2+} . Furthermore, to correlate these results to changes in EGFR and Neu expression and/or activation state, mRNAs, total and phosphorylated protein levels were also measured in both cell lines. In conclusion, our finding suggest that Ni^{2+} exposure may differently regulate apoptosis initiation in two epithelial cell lines derived from the human respiratory tract and support the potential involvement of EGFR and Neu receptor in mediating this effect.

2. Materials and methods

2.1. Cell cultures

Human alveolar type 2-like (A549) and bronchial epithelial cells (Beas-2B) were purchased from ATCC (Cat No. CCL-185 and CRL-9609, respectively). Both cell lines were maintained in epidermal growth factor (EGF)-free Dulbecco modified Eagle medium (DMEM) containing 500 mg/L glucose, L-glutamine, 100 mg/L sodium pyruvate supplemented with 10% FBS, 0.02 M/L HEPES, 100 U/mL penicillin, and 50 ng/mL streptomycin. Cells were grown in an incubator at 37 °C in a humidified atmosphere with 5% CO_2 and passaged at 80% confluence.

2.2. Cell viability (MTT assay)

To assess cell viability, we used the cell proliferation kit I (MTT) following manufacturer's instructions (Roche). Cells were seeded into 96-well plates at a concentration of 1×10^4 cells/well and allowed to adhere for 24 h. Cells were then treated either with a range of concentrations (0, 0.1, 0.5, 1, 2.5 and 5 mM, respectively) of nickel acetate (Ni^{2+}) (Sigma–Aldrich) for 24 h for dose–response analyses or with 0.1 mM Ni^{2+} for 24, 48, 72 h and 1 week for time-course analyses. EGF-free DMEM containing 0.5 mg/mL 3-[4,5-dimethylthiazol-2-yl]-2,5-diphenyltetrazolium bromide (MTT) (Sigma–Aldrich) was added in each well. Following incubation for 4 h at 37 °C, medium was removed, and 100 μL of DMSO was added. Formazan formed by the cleavage of the yellow tetrazolium salt MTT was measured spectrophotometrically by absorbance change at 550–600 nm using a microplate reader.

2.3. Apoptotic assay by immunodetection of oligonucleosomes

Mononucleosomes and oligonucleosomes released from the nucleus into the cytoplasm of apoptotic cells were detected with

the use of a sandwich enzyme-linked immunosorbent assay (The Cell Death Detection) ELISA^{PLUS} 10 \times (Roche Applied Sciences). The assay is based on quantitative sandwich enzyme-linked immunosorbent assay principle, with mouse monoclonal antibody direct against DNA histones, respectively. For sample preparation, both A549 and Beas-2B cells treated with 0.1 mM Ni^{2+} for 24, 48, 72 h and 1 week were harvested by trypsinization. Cells were lysed in incubation buffer for 30 min. The lysate was then centrifuged at 20,000g \times 10 min. Supernatant was diluted to yield 1×10^4 cell equivalents/mL and used for immunodetection. The assay was performed as follows: (1) an antibody that react with the histone H1, H2A, H2B, H3 and H4 was fixed on the wall of the microplate module provided with the kit; (2) samples prepared as described above were added to the plate containing the immobilized anti-histone antibody; (3) anti-DNA monoclonal antibodies conjugated to peroxidase were added, to allow their binding to the DNA part of nucleosomes; and (4) after removal of unbound peroxidase conjugate, the amount of peroxidase retained in the immunocomplex was determined photometrically with 2,2'-azino-di(3-ethylbenzthiazoline sulfonate) as a substrate.

2.4. Hoechst 33258 nuclear staining

A549 and Beas-2B cells were exposed to 0.1 mM Ni^{2+} for 24 and 48 h. The typical morphological features of apoptotic degeneration were analyzed by the use of fluorescence microscopy with the nuclear dye Hoechst 33258 (Forloni et al., 1993). Cells were fixed with a solution of methanol/acetic acid (3:1 v/v) for 30 min, washed three times in PBS and incubated for 15 min at 37 °C with 0.4 $\mu\text{g}/\text{mL}$ Hoechst 33258 dye. After being rinsed in water, cells were visualized for determination of nuclear chromatin morphology with the use of an Axiovert 40 fluorescence microscope (Carl Zeiss Inc.). Apoptotic cells were recognized on the basis of nuclear condensation and/or fragmented chromatin. Each condition was reproduced in three dishes per experiment. Both apoptotic and normal cells were determined by analyzing at least three different fields per dish in a fixed pattern.

2.5. Analysis of mRNA expression by RT-PCR

Total RNA extracts obtained from untreated A549 and Beas-2B cells were isolated by 1 mL TRIzol reagent (Invitrogen) and 0.2 mL chloroform and precipitated with 0.5 mL isopropanol. Pellet was washed with 75% ethanol and air dried. Single stranded cDNAs were synthesized incubating total RNA (5 μg) with SuperScript III RNase H-reverse transcriptase (200 U/ μL) (Invitrogen); Oligo-(dT)₂₀ primer (100 nM) (Invitrogen); 1 mM dNTP mix (Invitrogen), dithiothreitol (DTT, 0.1 M), Recombinant RNase-inhibitor (40 U/ μL) at 42 °C for 1 h in a final volume of 20 μL . Reaction was terminated by incubation of samples at 70 °C for 10 min. Aliquots of cDNA were amplified using specific primers for EGFR receptor, Neu receptor and S18 ribosomal subunit. Oligonucleotide sequences are listed in Table 1. Each PCR reaction contained 0.4 μM specific primers, 200 μM dNTPs, 1.25 U AmpliTaq Gold DNA polymerase and GeneAmp buffer containing 2.5 mM MgCl_2^{2+} (Applied Biosystem). PCR was performed using the following three cycle programs: (I) denaturation of cDNA (1 cycle: 95 °C for 12 min); (II) amplification (40 cycles: 95 °C for 30 s, 60 °C for 30 s, 72 °C for 45 s); (III) final extension (1 cycle: 72 °C for 7 min). Amplification products were separated by electrophoresis in a 1.8% agarose gel in 0.045 M Tris–borate/1 mM EDTA (TBE) buffer.

2.6. Real-time quantitative PCR analysis

Aliquots of cDNA (400 ng) from either untreated or 0.1 mM Ni^{2+} -treated A549 and Beas-2B cells at different times (24 and

Table 1
Primer sequences.

Gene	Forward primer	Reverse primer	Bp
EGFR Acc # NM005228.3	GTTGAGGGCAATGAGGACAT	AACTGTGAGGTGGTCCTGG	114
Neu Acc # NM00448.2	CCCACGTCCGTAGAAAGGTA	ACAGTGGCATCTGTCACTG	148
S18 Acc # NM022551.2	GGACCTGGCTGATTTCCTCA	GAGGATGAGGTGGAACGTGT	115

Forward and reverse primers were selected from the 5' and 3' region of each gene mRNA. The expected length of PCR products is indicated in the right column.

48 h, respectively) were amplified in parallel reactions with external standards at known amounts (purified PCR products, ranging from 10^2 to 10^8 copies) using specific primer pairs listed in Table 1. To normalize data, mRNA levels of the S18 ribosomal subunit (reference gene) were measured in each amplification. Each PCR reaction (final volume of 20 μ L) contained 0.5 μ M primers, 1.6 mM Mg^{2+} , $1 \times$ Light Cycler-FastStart DNA Master SYBR Green I (Roche Diagnostic). Amplifications were performed using a Light Cycler 1.5 instrument (Roche Diagnostic) with the following program setting: (I) cDNA denaturation (1 cycle: 95 °C for 10 min); (II) quantification (45 cycles: 95 °C for 10 s, 57 °C for 7 s, 72 °C for 5 s); (III) melting curve analysis (1 cycle: 95 °C for 0 s, 65 °C for 15 s, 95 °C for 0 s); (IV) cooling (1 cycle: 40 °C for 30 s). Each amplification was carried out in duplicate in at least three different experiments. The temperature transition rate was 20 °C/s, except for the third segment of the melting curve analysis where it was set to 0.1 °C/s. Quantification was obtained by comparing the fluorescence emitted by PCR products at unknown concentration with the fluorescence emitted by external standards at known concentration. For this analysis, fluorescence values, measured in the log-linear phase of amplification, were estimated with the second derivative maximum method using Light Cycler Data Analysis software. PCR products specificity was evaluated by melting curve analysis followed by gel electrophoresis.

To assess the different expression levels we employed the well-established Δ Ct comparative method (Schmittgen and Livak, 2008). We analyzed the mean of the crossing points (or crossing threshold = Ct) of each sample. The Ct represents the number of cycles needed to detect a fluorescence above a specific threshold level and it is inversely correlated to the amount of nucleic acids template present in the reaction. The Δ Ct was calculated by normalizing the mean Ct of each sample to the mean Ct of the reference gene measured in the same experimental conditions. For quantification of each gene we considered either untreated A549 or Beas-2B cultures as positive samples (calibrator sample). The $\Delta\Delta$ Ct of each sample was calculated by subtracting calibrator Δ Ct to sample Δ Ct. The formula $2^{-\Delta\Delta Ct}$ was used to calculate the fold change.

2.7. Western blot analysis

Crude extracts were prepared by homogenizing cells in a buffer containing 20 mM Tris (pH 7.4), 2 mM EDTA, 0.5 mM EGTA; 50 mM mercaptoethanol, 0.32 mM sucrose and a protease inhibitor cocktail (Roche Diagnostics) supplemented with phosphatase inhibitors (Roche Diagnostics) using a Teflon-glass homogenizer and then sonicated. Protein concentrations were determined by Bradford's method (Bradford, 1976) using BSA as a standard. Sample proteins (50 μ g) were diluted in 4 \times sodium dodecyl sulfate (SDS) protein gel loading solution (Invitrogen), boiled for 10 min, separated on 4–12% Bis–Tris gel (Invitrogen) by electrophoresis and processed as previously described by Pascale et al., 1996.

Immunoblot analysis was performed by using polyclonal antibodies listed below: rabbit polyclonal IgG raised against a peptide mapping at the C-terminus of EGFR of human origin (sc-03, Santa

Cruz Biotechnology, Inc.), rabbit polyclonal IgG raised against epitope corresponding to phosphorylated Tyr 1173 of EGFR of human origin (sc-03, Santa Cruz Biotechnology, Inc.), mouse monoclonal raised against the extracellular domain of Neu of human origin (sc-74241, Santa Cruz Biotechnology, Inc.), rabbit polyclonal IgG raised against epitope corresponding to a short amino acid sequence containing phosphorylated Tyr 1248 of Neu of human origin (sc-12352, Santa Cruz Biotechnology, Inc.), mouse monoclonal IgG₁ raised against a synthetic peptide corresponding to amino acids 41–54 of human Bcl-2 (sc-509, Santa Cruz Biotechnology, Inc.), rabbit polyclonal IgG, raised against a epitope mapping at the N-terminus of BAX of human origin (sc-493, Santa Cruz Biotechnology, Inc.) and rabbit polyclonal IgG raised against epitope corresponding to amino acids 210–444 mapping at the C-terminus of β -tubulin of human origin (sc-9104, Santa Cruz Biotechnology, Inc.) which was used as loading control. All primary antibodies were diluted 1:200, while secondary antibodies (HRP-conjugated goat anti-mouse and anti-rabbit antibodies, Amersham Biosciences) were used at 1:10000. Blots were developed using enhanced chemiluminescence technique (Amersham Biosciences). No signal was detected when the primary antibody was omitted (data not shown).

2.8. Statistical analysis

Statistical analysis was performed using GraphPad InStat version 3.00, GraphPad Software Inc., San Diego CA, USA). Paired comparisons were performed using the two-tailed Student *t*-test. One-way analysis of variance (ANOVA) was used to compare differences among three or more data sets and statistical significance was assessed by Tukey–Kramer post hoc test, unless otherwise indicated. The level of significance accepted for all statistical tests was $p \leq 0.05$.

3. Results

3.1. Dose–response effect of Ni²⁺ treatment on cell viability in A549 and Beas-2B cells

To investigate the effect of Ni²⁺ treatment on cell viability, both A549 and Beas-2B cells were exposed to increasing concentrations of Ni²⁺ (0, 0.1, 0.5, 1, 2.5 and 5 mM, respectively) for 24 h and MTT analyses were performed. As indicated in Fig. 1, exposure to Ni²⁺ decreased cell viability in a dose-dependent manner in A549 but not in Beas-2B cells. In particular, with respect to untreated controls, percentage of cell viability in A549 cells was significantly reduced already at 0.1 mM Ni²⁺ ($*p < 0.05$ Vs Control, ANOVA followed by Tukey–Kramer post hoc test) and further declined with higher Ni²⁺ concentrations (0.5, 1, 2.5 and 5 mM, respectively, $***p < 0.001$ Vs Control). Conversely, Beas-2B cells showed reduced susceptibility to Ni²⁺ treatment, with cell viability being significantly reduced only at concentrations ≥ 1 mM ($**p < 0.01$ or $***p < 0.001$ Vs Control). Furthermore, comparative analyses revealed that Ni²⁺-induced differences in cell viability between the two cell lines reached statistical significance at 0.1 mM Ni²⁺ ($\#p < 0.05$ Vs Ni²⁺-treated A549 cells)

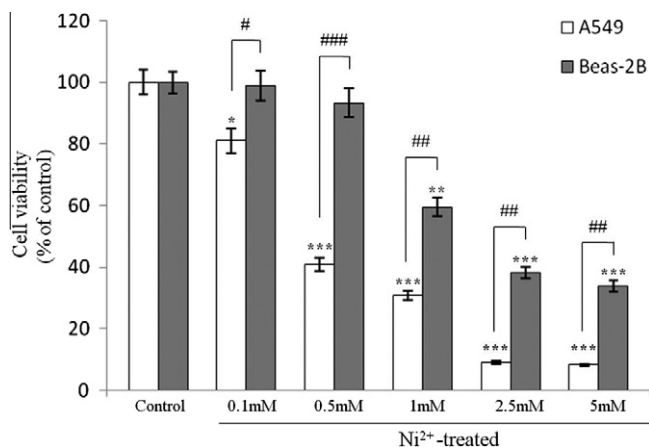


Fig. 1. Dose–response effect of Ni²⁺ treatment on cell viability in A549 and Beas-2B cells. Cell viability was assessed in A549 and Beas-2B cells exposed to increasing concentrations of Ni²⁺. Cells were treated with a range of concentrations (0, 0.1, 0.5, 1, 2.5 and 5 mM) of Ni²⁺ for 24 h and processed for MTT measurements as described in Section 2. Values are expressed as percentage of cell viability in untreated controls ($n = 3$) \pm SD. Results are representative of three independent experiments. * $p < 0.05$, ** $p < 0.01$ or *** $p < 0.001$ Vs untreated cells; # $p < 0.05$, ## $p < 0.01$ or ### $p < 0.001$ Vs Ni²⁺-treated A549 cells (One-Way ANOVA followed by Tukey post hoc test).

and further increased at higher concentrations (## $p < 0.01$ or ### $p < 0.001$ Vs Ni²⁺-treated A549 cells) (Fig. 1).

3.2. Time-course of Ni²⁺-induced effects on cell viability in A549 and Beas-2B cells

To evaluate the effects of Ni²⁺ exposure on cell viability over time, MTT analyses were carried out either in untreated A549 or Beas-2B cells (Control) or cells exposed to 0.1 mM Ni²⁺ for 24, 48, 72 h and 1 week. Our finding demonstrated that a relatively low concentration of Ni²⁺ (0.1 mM) was sufficient to cause significant reduction of cell viability in A549 cells at every time point considered, reaching the maximum effect after 72 h (*** $p < 0.001$ Vs Control, unpaired Student *t*-test) (Fig. 2A). Oppositely, Beas-2B cells survival rate was not affected by 0.1 mM Ni²⁺ exposure neither

after 24 and 48 h, whereas a significant reduction was observed after 72 h and 1 week (* $p < 0.05$ and ** $p < 0.01$ Vs Control, respectively) (Fig. 2B). These results suggested that Beas-2B cells might be more resistant to Ni²⁺-induced cell death than A549.

3.3. Oligonucleosomes formation and DNA damage in Ni²⁺-treated A549 and Beas-2B cells

To establish whether the previously observed effects of Ni²⁺ treatment on cell viability in A549 and Beas-2B cells could be associated to the activation of an apoptotic process we performed an enzyme-linked immunosorbent assay for the detection of mono-/oligonucleosomes. A549 and Beas-2B cells were treated with 0.1 mM Ni²⁺ for the indicated times and apoptotic levels were measured. We found that in Ni²⁺-treated A549 cells apoptosis was significantly increased as compared to control (untreated cells at time 0) both after 24 and 48 h (* $p < 0.05$ Vs Control; ANOVA followed by Tukey–Kramer post hoc test). Prolonged exposure to Ni²⁺ (72 h and 1 week, respectively) further increased apoptotic levels in A549 cells (** $p < 0.01$ Vs Control) (Fig. 3A). In contrast to A549 cells, Ni²⁺ treatment was not able to trigger apoptosis in Beas-2B cells after 24 and 48 h, but required longer periods of exposure (72 h and 1 week, respectively) to produce a significant increase in apoptotic levels (* $p < 0.05$ and ** $p < 0.01$ Vs Control) (Fig. 3A). Evidence of a disparity in apoptotic response to Ni²⁺ treatment between the two cell lines was also confirmed statistically, showing significant changes in oligonucleosome formation between Ni²⁺-treated Beas-2B and A549 cells (# $p < 0.05$ Vs Ni²⁺-treated A549 cells at the indicated times) (Fig. 3A). To provide morphological evidence of DNA damage, either untreated or 0.1 mM Ni²⁺-treated A549 and Beas-2B cells were stained with the Hoechst 33342 nuclear dye (Fig. 3B). After 24 and 48 h treatment, A549 cells exposed to Ni²⁺ showed evident signs of DNA damage with respect to untreated controls, whereas apparent normal morphology persisted in Ni²⁺-treated Beas-2B cells (Fig. 3B).

3.4. Identification of EGFR and Neu receptor mRNAs in A549 and Beas-2B cells

RT-PCR analysis was performed both in A549 and Beas-2B cells to evaluate whether these cell lines express EGFR and Neu receptor

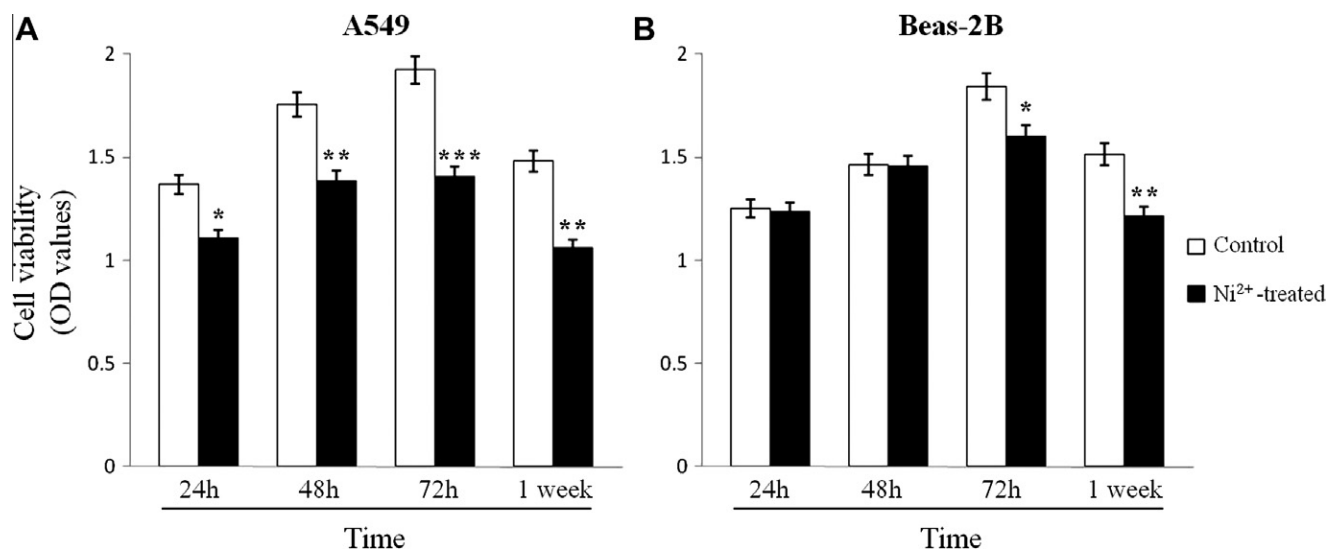


Fig. 2. Time-course of Ni²⁺-induced effects on cell viability in A549 and Beas-2B cells. Cell viability was measured in A549 (A) and Beas-2B cells (B) exposed to 0.1 mM Ni²⁺ at different time points (24, 48, 72 h and 1 week, respectively). Untreated (Control) or Ni²⁺-treated cells at the indicated times were processed for MTT measurements as detailed in Section 2. Values are expressed as mean ODs ($n = 3$) \pm SD. Results are representative of three independent experiments. * $p < 0.05$, ** $p < 0.01$ or *** $p < 0.001$ Vs Control at the indicated time (two-tailed Student *t*-test).

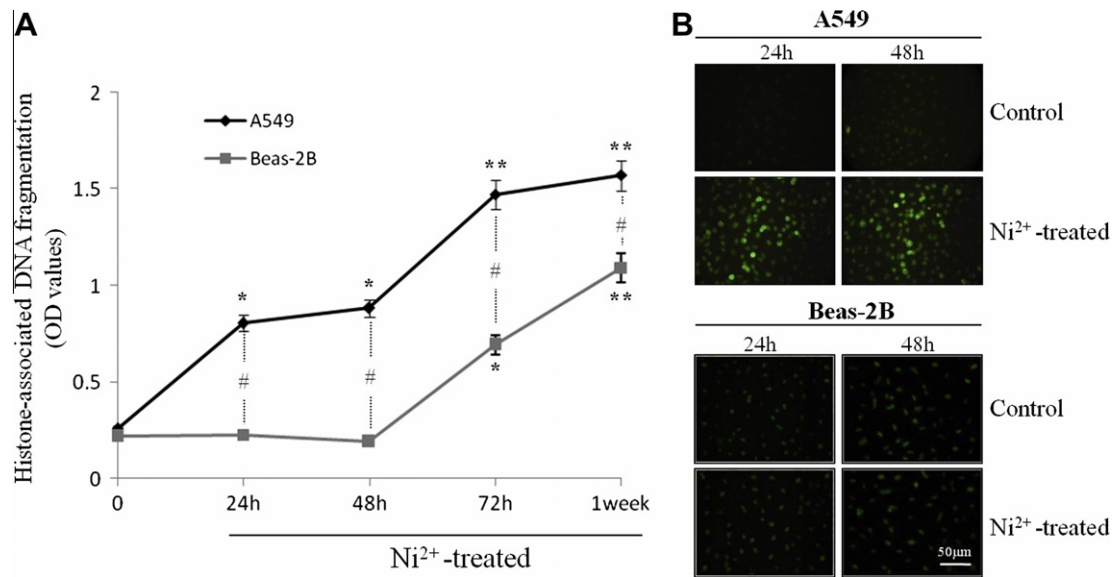


Fig. 3. Oligonucleosomes formation and DNA damage in Ni^{2+} -treated A549 and Beas-2B cells. Effect of Ni^{2+} exposure on apoptosis in A549 and Beas-2B cells as determined by oligonucleosomes detection (A) and Hoechst 33258 nuclear staining (B). (A) Cells were treated with 0.1 mM Ni^{2+} for indicated times and processed for oligonucleosomes detection as described in Section 2. Values are expressed as mean ODs ($n = 3$) \pm SD. Oligonucleosomes formation in untreated cells is indicated as time point 0. * $p < 0.05$ or ** $p < 0.01$ Vs untreated cells; # $p < 0.05$ Vs Ni^{2+} -treated A549 cells (One-Way ANOVA followed by Tukey post hoc test). (B) Representative photomicrographs showing the effect of Ni^{2+} treatment (Ni^{2+} -treated) on DNA damage in A549 and Beas-2B cells after 24 and 48 h. Untreated cells are indicated as Control. Cells were stained with the fluorescent nuclear dye Hoechst 33258 and viewed at 40 \times magnification. Results shown are representative of three independent experiments. Scale bar = 50 μm .

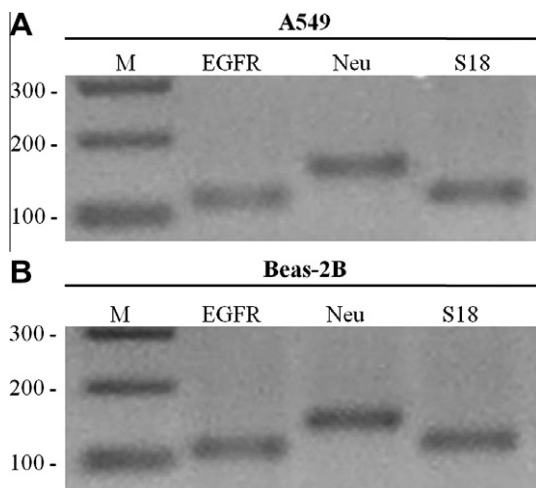


Fig. 4. Identification of EGFR and Neu receptor mRNAs in A549 and Beas-2B cells. Amplification products obtained using specific primer pairs (Table 1) demonstrated that both EGFR and Neu receptor genes are expressed in both A549 and Beas-2B cells (Fig. 4). Primers for the constitutively expressed S18 ribosomal subunit were used as control in each PCR amplification and generated bands of the expected length. A 100-bp DNA ladder is shown on the left side of each gel (lane M) with bands labeled in bp units.

mRNAs. Amplification products obtained using specific primer pairs (Table 1) demonstrated that EGFR and Neu receptor genes are expressed in both cell lines (Fig. 4). Primers for the constitutively expressed S18 ribosomal subunit were used as control in each PCR amplification and generated bands of the expected length.

3.5. EGFR and Neu receptor mRNA expression in Ni^{2+} -treated A549 and Beas-2B

To investigate whether Ni^{2+} treatment affected either EGFR and/or Neu receptor expression, both A549 and Beas-2B were treated

with 0.1 mM Ni^{2+} for 24 and 48 h and subsequently transcript levels were measured by quantitative real-time PCR analyses. Our findings indicate that EGFR and Neu receptor genes were differentially affected by Ni^{2+} exposure in either cell line after 24 and 48 h (Table 2). Data obtained from these analyses showed that, as compared to untreated controls, EGFR and Neu expression levels were significantly decreased with treatment in A549 cells (* $p < 0.05$ or ** $p < 0.01$ Vs Control, ANOVA followed by Dunnett's post hoc test) (Table 2). Conversely, Ni^{2+} -treated Beas-2B cells showed a significant increase in both genes mRNAs after 24 h (** $p < 0.01$ Vs Control), whereas such significant increase in gene expression was evident for Neu receptor (** $p < 0.01$ Vs Control) but not for EGFR after 48 h.

3.6. EGFR and Neu activation, Bcl-2 and BAX expression in A549 and Beas-2B exposed to Ni^{2+}

Western blot analyses were performed to examine the effects of Ni^{2+} treatment on EGFR and Neu receptor protein levels as well as in their phosphorylated forms both in A549 and Beas-2B cells after 24 and 48 h. Cells were maintained either in EGF-free medium (Ctrl), treated with 100 ng/mL EGF (Sigma) (positive control, +EGF) or exposed to 0.1 mM Ni^{2+} (Ni^{2+} -treated) at the indicated times. As displayed in Fig. 5, total EGFR and Neu receptor protein expression showed high correspondence with mRNA measurements, although a correlation between transcript and protein levels may not always be found (Sonenberg and Hinnebusch, 2009). Interestingly, the expression of phosphorylated proteins (p-EGFR and p-Neu, respectively) was oppositely regulated by Ni^{2+} exposure in the two cell lines (Fig. 5A). More specifically, in A549 cells, both p-EGFR and p-Neu expression was downregulated in response to Ni^{2+} treatment after 24 and 48 h, whereas in Beas-2B cells, treatment upregulated both p-EGFR and p-Neu expression (Fig. 5A), suggesting that Ni^{2+} might differentially regulate EGFR and Neu activation state in the two cell lines. To find a potential correlation between the expression of phosphorylated proteins and the triggering of apoptosis after metal treatment, the expression of the antiapoptotic protein Bcl-2 and the proapoptotic protein BAX were also analyzed in both cell lines. As demonstrated in Fig. 5B,

Table 2
Identification of EGFR and Neu receptor mRNAs in A549 and Beas-2B cells.

Cell line	Gene	Treatment		
		Control (untreated) Mean fold change \pm SEM	Ni ²⁺ -treated after 24 h	Ni ²⁺ -treated after 48 h
A549	EGFR	1.00 \pm 0.11	0.7 \pm 0.12*	0.54 \pm 0.04**
	Neu	1.04 \pm 0.14	0.34 \pm 0.06**	0.73 \pm 0.08*
Beas-2B	EGFR	1.02 \pm 0.12	1.59 \pm 0.04**	1.14 \pm 0.06
	Neu	1.03 \pm 0.10	1.40 \pm 0.06**	1.51 \pm 0.09**

A549 and Beas-2B cells were either left untreated (Control) or treated with 0.1 mM Ni²⁺ for 24 and 48 h. EGFR and Neu receptors mRNAs were measured by quantitative real-time PCR analysis as described in Section 2. Results are presented as mean fold change of control groups (Control, $n = 3$) \pm SEM. Relative fold changes of target genes obtained after normalization to the endogenous ribosomal protein S18 (housekeeping gene) were calculated according to the comparative Δ Ct method (Schmittgen and Livak, 2008). Baseline expression levels of the control groups were set to 1. Results are representative of three independent experiments, each run in duplicate.

* $p < 0.05$.

** $p < 0.01$ Vs Control (One-Way ANOVA followed by Dunnett's post hoc test).

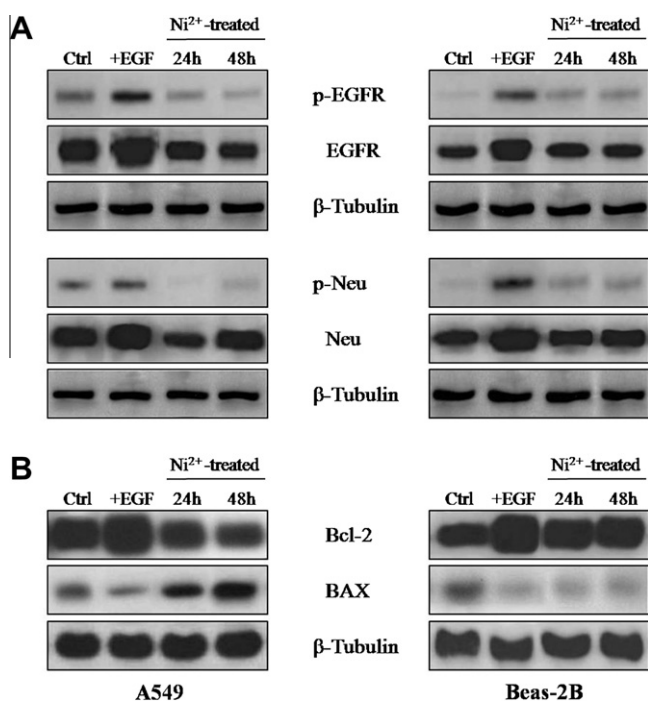


Fig. 5. EGFR and Neu activation, Bcl-2 and BAX expression in A549 and Beas-2B exposed to Ni²⁺. Western blot analyses showing Ni²⁺-induced changes in the expression of total and phosphorylated EGFR and Neu receptor protein (A) as well as Bcl-2 and BAX expression (B) in A549 and Beas-2B after 24 and 48 h. Representative immunoblots were obtained using 50 μ g of cell homogenates from either untreated (Ctrl), 100 ng/mL EGF-treated (positive control, +EGF) or Ni²⁺-treated A549 and Beas-2B cells at the indicated times. β -Tubulin was used as loading control in each experiment. The results are representative of at least three independent determinations.

Ni²⁺-treated A549 cells showed decreased Bcl-2 and increased BAX expression both after 24 and 48 h, whereas in Beas-2B cells, Ni²⁺ caused the induction of the antiapoptotic Bcl-2 and markedly reduced BAX expression, implying a possible inverse correlation between EGFR/Neu phosphorylation levels and the activation of the intrinsic apoptotic pathway.

4. Discussion

The correlation between nickel compounds exposure and increased risk of human respiratory cancer has been widely reported in epidemiologic studies (Kasprzak et al., 2003). However, the exact mechanisms of nickel-induced carcinogenesis are not yet clearly understood. Since inhalation is one of the main occupational

exposure routes of nickel exposure (Costa, 2002; Sivulka, 2005), human alveolar type 2-like (A549) and human bronchial epithelial cells (Beas-2B) were used in this study. These are well-established cell lines and have been extensively used to investigate the effects of environmental pollutants (Wilson et al., 2000; Laan et al., 2004; Kawasaki et al., 2001).

In the present study we have shown that Ni²⁺ exposure differentially affected both cell viability and apoptosis in two distinct airway epithelial cell lines. More specifically, we found that at relatively low concentrations (0.1 and 0.5 mM), Ni²⁺ exposure significantly reduced cell viability (Figs. 1 and 2) and increased apoptosis and DNA damage in A549 cells (Fig. 3). Oppositely, equivalent concentrations of the metal were not able to produce any significant biological effect in cell viability and apoptosis in Beas-2B cells (Figs. 1–3), indicating, at least in part, a decreased susceptibility of bronchial compared to alveolar epithelial cells to Ni²⁺-induced cell death. These results are consistent with previous finding showing the effect of nickel in different cell lines, which demonstrated that the metal either promoted apoptosis resistance in Beas-2B cells (Ding et al., 2006; Pan et al., 2011) or induced apoptosis in other cell lines, like T cell hybridoma cells, Jurkat cells, and mouse epidermal JB6 cells (Shiao et al., 1998; Kim et al., 2002; Zhao et al., 2009). However, the molecular mechanisms by which nickel might trigger apoptosis in some cell types and not in others remain to be fully understood. According to literature data, reactive oxygen species (ROS) generation (Salnikow et al., 1994; Pan et al., 2010), transcription factor activation (Cruz et al., 2004; Salnikow et al., 2003) as well as hypermethylation (Lee et al., 1995) are the main events that occur in nickel-induced carcinogenesis. Nonetheless, it has also been postulated that nickel compounds might also have a role in the regulation of sets of genes important in normal growth control (Mollerup et al., 1996). Based on these finding, we sought to investigate whether the different sensitivity of cells to nickel treatment could be associated to a differential regulation in the expression and activation state of two members of the EGF receptor family, termed EGFR and Neu. These receptors have been shown to be differently regulated after exposure to different metals both in A549 and Beas-2B cells, thus activating molecular pathways that either promoted proliferation or induced cell death (Wu et al., 1999; Castorina et al., 2008; Kundu et al., 2011). Here we showed that exposure of A549 cells to subtoxic doses of Ni²⁺ reduced both total EGFR and Neu mRNA and protein expression, as well as their respective phosphorylated proteins, whereas induction of gene and protein expression and a concurrent increase in the activation state of EGFR and Neu were observed in Ni²⁺-exposed Beas-2B cells (Table 2 and Fig. 5A), although increased phosphorylation could not be associated with promotion of cell proliferation. The latter finding is supported by previous reports indicating that agents other than EGF family member ligands may induce EGF/Neu receptor tyrosine

phosphorylation (Li et al., 1998; Zwick et al., 1997) and that nickel may induce apoptosis resistance in Beas-2B cells without affecting cell growth (Ding et al., 2006). Our data showing that Ni²⁺ exposure can activate these two EGF receptors in Beas-2B cells are similar to previous findings by Chen et al., 1998 who observed the role of EGFR in mediating arsenite-induced protein tyrosine phosphorylation in pheochromocytoma cells. Although the mechanism responsible for metal-induced activation of EGF receptor tyrosine kinase is unknown, it is possible that nickel may directly interact with the EGF receptor molecules, causing a structural alteration or dimerization that results in activation of the kinase domain. A further explanation for the decreased/increased expression of p-EGFR and p-Neu in A549 and Beas-2B cells could be that nickel acts by either activating or inactivating phosphatases that serve to dephosphorylate EGFR and Neu, allowing the phosphorylated forms to accumulate. Alternatively, it is possible that nickel-induced ROS generation may vary among different cell types, ultimately leading to membrane changes that can either promote or reduce receptor activation, hence causing either inactivation or activation of apoptosis. Although further studies are required to confirm these possibilities, both nickel-induced phosphatase- and ROS-dependent potential effects on receptors activation represent a plausible explanation for the differential effects of nickel in A549 and Beas-2B cells. However, since we found that subtoxic nickel exposure decreased the expression of the antiapoptotic Bcl-2 protein and increased BAX protein levels in A549 cells, whereas it increased Bcl-2 and decreased BAX expression in Beas-2B cells (Fig. 5B), we also suggest that changes in levels of phosphorylated EGFR and Neu may potentially involve the intrinsic apoptotic pathway.

Conflict of interest

None declared.

Acknowledgements

This study was supported and funded by the National Institute for Occupational Safety and Prevention – ISPESL (Italy). Grant No. B01-DML-07.

We thank Mr. Pietro Asero for his technical support and Dr. Francesco Murabito for the administrative support.

References

- Ahamed, M., 2011. Toxic response of nickel nanoparticles in human lung epithelial A549 cells. *Toxicol. In Vitro* 25, 930–936.
- Baselga, J., Arteaga, C.L., 2005. Critical update and emerging trends in epidermal growth factor receptor targeting in cancer. *J. Clin. Oncol.* 23, 2445–2459.
- Bradford, M.M., 1976. A rapid and sensitive method for the quantitation of microgram quantities of protein utilizing the principle of protein-dye binding. *Anal. Biochem.* 72, 248–254.
- Cangul, H., Broday, L., Salnikow, K., Sutherland, J., Peng, W., Zhang, Q., Poltaratsky, V., Yee, H., Zoroddu, M.A., Costa, M., 2002. Molecular mechanisms of nickel carcinogenesis. *Toxicol. Lett.* 127, 69–75.
- Castorina, A., Tiralongo, A., Cavallo, D., Loreto, C., Carnazza, M.L., Iavicoli, S., D'Agata, V., 2008. Expression profile of ErbB receptor's family in human alveolar type 2-like cell line A549 exposed to hexavalent chromium. *Toxicol. In Vitro* 22, 541–547.
- Chen, W., Martindale, J.L., Holbrook, N.J., Liu, Y., 1998. Tumor promoter arsenite activates extracellular signal-regulated kinase through a signaling pathway mediated by epidermal growth factor receptor and Shc. *Mol. Cell. Biol.* 18, 5178–5188.
- Correa, P., Mark, J.S., 1998. Miller. Carcinogenesis, apoptosis and cell proliferation. *Br. Med. Bull.* 54, 151–162.
- Costa, M., 2002. Molecular mechanisms of nickel carcinogenesis. *Biol. Chem.* 383, 961–967.
- Cruz, M.T., Gonçalves, M., Figueiredo, A., Carvalho, A.P., Duarte, C.B., Lopes, M.C., 2004. Contact sensitizer nickel sulfate activates the transcription factors NF-κB and AP-1 and increases the expression of nitric oxide synthase in a skin dendritic cell line. *Exp. Dermatol.* 13, 18–26.
- Denkhaus, E., Salnikow, K., 2002. Nickel essentiality, toxicity, and carcinogenicity. *Crit. Rev. Oncol. Hematol.* 42, 35–36.
- Ding, J., Zhang, X., Li, J., Song, L., Ouyang, W., Zhang, D., Xue, C., Costa, M., Meléndez, J.A., Huang, C., 2006. Nickel compounds render anti-apoptotic effect to human bronchial epithelial Beas-2B cells by induction of cyclooxygenase-2 through an IKKβ/p65-dependent and IKKα- and p50-independent pathway. *J. Biol. Chem.* 281, 39022–39032.
- Forloni, G., Angeretti, N., Chiesa, N., Monzoni, E., Salmona, M., Bugiani, O., Tagliavini, F., 1993. Neurotoxicity of a prion protein fragment. *Nature* 362, 543–546.
- Kasprzak, K.S., Sunderman, J.F.W., Salnikow, K., 2003. Nickel carcinogenesis. *Mutat. Res.* 533, 67–97.
- Kawasaki, S., Takizawa, H., Takami, K., Desaki, M., Okazaki, H., Kasama, T., Kobayashi, K., Yamamoto, K., Nakahara, K., Tanaka, M., Sagai, M., Ohtoshi, T., 2001. Benzene-extracted components are important for the major activity of diesel exhaust particles—effect on interleukin-8 gene expression in human bronchial epithelial cells. *Am. J. Respir. Cell Mol. Biol.* 24, 419–426.
- Kim, K., Lee, S.H., Seo, Y.R., Perkins, S.N., Kasprzak, K.S., 2002. Nickel(II)-induced apoptosis in murine T cell hybridoma cells is associated with increased fas ligand expression. *Toxicol. Appl. Pharmacol.* 185, 41–47.
- Kundu, S., Sengupta, S., Bhattacharya, A., 2011. EGFR upregulates inflammatory and proliferative responses in human lung adenocarcinoma cell line (A549), induced by lower dose of cadmium chloride. *Inhal. Toxicol.* 23, 339–348.
- Laan, M., Bozinovski, S., Anderson, G., 2004. Cigarette smoke inhibits lipopolysaccharide-induced production of inflammatory cytokines by suppressing the activation of activator protein-1 in bronchial epithelial cells. *J. Immunol.* 173, 4164–4170.
- Lee, Y.W., Klein, C.B., Kargacin, B., Salnikow, K., Kitahara, J., Dowjat, K., Zhitkovich, A., Christie, N.T., Costa, M., 1995. Carcinogenic nickel silences gene expression by chromatin condensation and DNA methylation: a new model for epigenetic carcinogens. *Mol. Cell. Biol.* 15, 2547–2557.
- Li, X., Lee, J.W., Graves, L.M., Earp, H.S., 1998. Angiotensin II stimulates ERK via two pathways in epithelial cells: protein kinase C suppresses a G protein-coupled receptor-EGF receptor transactivation pathway. *EMBO J.* 17, 2574–2583.
- Liu, Z.G., Lewis, J., Wang, T.H., Cook, A., 2001. Role of c-Jun N-terminal kinase in apoptosis. *Methods Cell Biol.* 66, 187–195.
- Mollerup, S., Rivedal, E., Moehle, L., Haugen, A., 1996. Nickel(II) induces alterations in EGF- and TGF-β1-mediated growth control during malignant transformation of human kidney epithelial cells. *Carcinogenesis* 17, 361–367.
- Mosesson, Y., Yarden, Y., 2004. Oncogenic growth factor receptors: implications for signal transduction therapy. *Semin Cancer Biol.* 14, 262–270.
- Olayioye, M.A., Neve, R.M., Lane, H.A., Hynes, N.E., 2000. The ErbB signaling network: receptor heterodimerization in development and cancer. *EMBO J.* 19, 3159–3167.
- Pan, J., Chang, Q., Wang, X., Son, Y., Zhang, Z., Chen, G., Luo, J., Bi, Y., Chen, F., Shi, X., 2010. Reactive oxygen species-activated Akt/ASK1/p38 signaling pathway in nickel compound-induced apoptosis in BEAS 2B cells. *Chem. Res. Toxicol.* 23, 568–577.
- Pan, J.J., Chang, Q.S., Wang, X., Son, Y.O., Liu, J., Zhang, Z., Bi, Y.Y., Shi, X., 2011. Activation of Akt/GSK3β and Akt/Bcl-2 signaling pathways in nickel-transformed BEAS-2B cells. *Int. J. Oncol.* 39, 1285–1294.
- Pascale, A., Fortino, I., Covoni, S., Trabucchi, M., Wetsel, W.C., Battaini, F., 1996. Functional impairment in protein kinase C by RACK1 (receptor for activated C kinase 1) deficiency in aged rat brain cortex. *J. Neurochem.* 67, 2471–2477.
- Salnikow, K., Gao, M., Voitkun, V., Huang, X., Costa, M., 1994. Altered oxidative stress responses in nickel-resistant mammalian cells. *Cancer Res.* 54, 6407–6412.
- Salnikow, K., Costa, M., 2000. Epigenetic mechanisms of nickel carcinogenesis. *J. Environ. Pathol. Toxicol. Oncol.* 19, 307–318.
- Salnikow, K., Davidson, T., Zhang, Q., Chen, L.C., Su, W., Costa, M., 2003. The involvement of hypoxia-inducible transcription factor-1-dependent pathway in nickel carcinogenesis. *Cancer Res.* 63, 3524–3530.
- Schmittgen, T.D., Livak, K.J., 2008. Analyzing real-time PCR data by the comparative C(T) method. *Nat. Protoc.* 3, 1101–1108.
- Shiao, Y.H., Lee, S.H., Kasprzak, K.S., 1998. Cell cycle arrest, apoptosis and p53 expression in nickel(II) acetate-treated Chinese hamster ovary cells. *Carcinogenesis* 19, 1203–1207.
- Sivulka, D.J., 2005. Assessment of respiratory carcinogenicity associated with exposure to metallic nickel: a review. *Regul. Toxicol. Pharmacol.* 43, 117–133.
- Sonenberg, N., Hinnebusch, A.G., 2009. Regulation of translation initiation in eukaryotes: mechanisms and biological targets. *Cell* 136, 731–745.
- Wilson, M.R., Stone, V., Cullen, R.T., Searl, A., Maynard, R.L., Donaldson, K., 2000. In vitro toxicology of respirable Montserrat volcanic ash. *Occup. Environ. Med.* 57, 727–733.
- Wu, W., Graves, L.M., Jaspers, I., Devlin, R.B., Reed, W., Samet, J.M., 1999. Activation of the EGF receptor signaling pathway in human airway epithelial cells exposed to metals. *Am. J. Physiol.* 277, 924–931.
- Wyllie, A.H., Bellamy, C.O., Bubb, V.J., Clarke, A.R., Corbet, S., Curtis, L., Harrison, D.J., Hooper, M.L., Toft, N., Webb, S., Bird, C.C., 1999. Apoptosis and carcinogenesis. *Br. J. Cancer* 1, 34–37.
- Yarden, Y., Sliwkowski, M.X., 2001. Untangling the ErbB signalling network. *Nat. Rev. Mol. Cell Biol.* 2, 127–137.
- Zandi, R., Larsen, A.B., Andersen, P., Stockhausen, M.T., Poulsen, H.S., 2007. Mechanisms for oncogenic activation of the epidermal growth factor receptor. *Cell Signal.* 19, 2013–2023.
- Zhao, J., Bowman, L., Zhang, X., Shi, X., Jiang, B., Castranova, V., Ding, M., 2009. Metallic nickel nano- and fine particles induce JB6 cell apoptosis through a

caspase-8/AIF mediated cytochrome c-independent pathway. J. Nanobiotechnol. 7, 2.
Zwick, E., Daub, H., Aoki, N., Yamaguchi-Aoki, Y., Tinhofer, I., Maly, K., Ullrich, A., 1997. Critical role of calcium-dependent epidermal growth factor receptor

transactivation in PC12 cell membrane depolarization and bradykinin signaling. J. Biol. Chem. 272, 24767–24770.